link.springer.com link.springer.com

Published online 14 February 2023 | https://doi.org/10.1007/s40843-022-2340-9
Sci China Mater 2023, 66(5): 2071–2078

Ultra-robust icephobic coatings with high toughness, strong substrate adhesion and self-healing capability

Yizhi Zhuo[1,5*], Verner Håkonsen[2], Siqi Liu[1], Tong Li[3], Feng Wang[1], Sihai Luo[4], Senbo Xiao[1], Jianying He[1*] and Zhiliang Zhang[1*]

ABSTRACT **Enabling surfaces with passive anti-icing properties is an emerging, facile, economical, and energy-saving strategy to mitigate the harm caused by ice accretion. However, the combination of icephobicity and robustness remains a daunting challenge. Herein, we present an ultra-robust transparent icephobic coating with high toughness, strong substrate adhesion, and self-healing capability. Hydrophobicity, smoothness, and softness of the coating guarantee low ice adhesion strength. By incorporating a spongy structure, the ice adhesion strength of the coating is lowered further down to 26.7 ± 1.1 kPa. Importantly, the coating exhibits high toughness, strong adhesion to the substrate, and self-healing capability due to the presence of multiple hydrogen bonding. Consequently, the coating maintains its icephobicity after 35 icing/deicing cycles and 600 abrasion cycles, is resilient to delamination, and is able to heal and recover its icephobicity from the mechanical damage introduced by both cuts and abrasions. Moreover, the coating sustains its icephobicity after eight months of immersion in saltwater, as well as exposure to the near-arctic weather in Trondheim (Norway). This work presents new insights into the design of robust icephobic coatings that can sustain severe mechanical loading for use in real complex environments.**

Keywords: robust, icephobic, adhesion, toughness, self-healing

INTRODUCTION

The excess accumulation of ice on the exposed surfaces of aircraft, ship hull, power line, pavement, windmill, and offshore platform, may cause enormous economic loss, as well as casualties [1–4]. Traditional active methods, such as the use of heating, mechanical force, and anti-freezing agents, have been applied to prevent ice accretion and protect infrastructure and transportation. Nevertheless, in general, these active processes are energy-intensive, time-consuming, costly, and environmentally harmful [5]. As an alternative strategy, using passive icephobic materials which can repel the incoming water droplets before freezing, delay or prevent ice formation, and reduce ice adhesion strength for easy removal by natural forces has drawn widespread attention [6–10].

Superhydrophobic surfaces (SHSs), which possess a chemical composition of low surface energy, combined with a hierarchical micro-nano structure, present a remarkable ability to repel water droplets and decrease ice adhesion strength [11–13]. However, vapor can condense within the micro-nano structure of SHS in a humid environment, which can lead to the formation of Wenzel-state water and ice, and thus induce mechanical interlocking which increases the ice adhesion strength considerably [14,15]. Moreover, durability is another critical issue that hampers the application of SHS for icephobicity, since the surface texture can be easily destroyed during ice removal and by abrasion [16]. Lubricant-infused surfaces display low ice adhesion strength because of the presence of a slippery liquid film on the surface; however, it is well known that this film can be depleted by ice and water [17]. Hydrophilic polymer networks, such as hydrophilic self-assembled monolayers [18], hydrogels [19,20], and ionogels [21], can suppress the ice formation and reduce the ice adhesion strength because their functional groups and ions can restrict the rearrangement of water molecules during freezing [22]. However, these functional groups and/or ions can be easily removed by mechanical wear and exhausted during cyclic applications, resulting in poor durability [20,21]. Hydrophobic soft coatings with sub-surface structures acting as macroscale crack initiators show ultralow ice adhesion strength, resulting from the formation of multiple cracks at the ice interface during loading due to deformation incompatibility [23–25]. However, mechanical robustness remains a common challenge to the current soft coatings [1,26]. This work reports an endeavor toward the development of robust icephobic materials that can sustain severe mechanical loading and harsh environments.

To design a robust icephobic coating (RIC), it is crucial to understand the failure process during deicing. As shown in Fig. 1, the detachment of ice from the surface can occur in the form of (i) cohesive failure of ice, (ii) adhesive failure between ice and the coating, (iii) cohesive failure of the coating, (iv) adhesive failure between the coating and substrate, or as a combination of them [27]. In order to continuously protect the surface from excessive ice accretion, adhesive failure between ice and the coating is favored, while the other three failure modes should be avoided (Fig. 1). Therefore, low ice adhesion strength is the key to ensure such an adhesive failure. Soft coatings are

[1] Nanomechanical Lab, Department of Structural Engineering, Norwegian University of Science and Technology (NTNU), Trondheim 7491, Norway
[2] NanoLab, Norwegian University of Science and Technology (NTNU), Trondheim 7491, Norway
[3] Ningbo Institute of Materials Technology and Engineering, Chinese Academy of Sciences, Ningbo 315201, China
[4] Department of Chemistry, Norwegian University of Science and Technology (NTNU), Trondheim 7491, Norway
[5] Institute of Solid State Physics, Hefei Institutes of Physical Science, Chinese Academy of Sciences, Hefei 230031, China
* Corresponding authors (emails: yizhi.zhuo@ntnu.no (Zhuo Y); jianying.he@ntnu.no (He J); zhiliang.zhang@ntnu.no (Zhang Z))

one of the best candidates since they demonstrate great promise for ultra-low ice adhesion [23,24]. The low ice adhesion strength of soft coatings is mainly attributed to the mismatch of the elastic modulus between ice and the coating [28]. It is known that the ice adhesion strength (τ) strongly correlates with Young's modulus (E) of the coating ($\tau \sim \sqrt{E}$) [29]. It should be noted that low modulus does not mean low mechanical endurance, which also depends on the toughness of the coating. A coating with high toughness shows enhanced wear resistance and can prevent cohesive failure during the icing/deicing process. In addition, strong adhesion between the coating and substrate is vital to avoid delamination, although only a few studies have focused on this topic [1].

Supramolecular silicones containing polydimethylsiloxane (PDMS) segments and reversible cross-linking segments, exhibit unique features of the intrinsic damage-healing function and tuneable mechanical properties, including stiffness and toughness [30–33]. Multiple hydrogen bonding has been introduced to serve as reversible cross-linking segments for enhancing the toughness of supramolecular silicones [34]. Most recently, supramolecular silicones with hydrogen bonding sites have also demonstrated strong adhesion to substrates, owing to the formation of hydrogen bonds at the interface [30,32]. These characteristics meet well with the requirement of RICs.

Herein, we present a supramolecular silicone elastomer containing octuple hydrogen bonding as the icephobic material (Fig. 1). The prepared RIC exhibits low ice adhesion strength, especially when a spongy structure is incorporated (26.7 ± 1.1 kPa). Thanks to the octuple hydrogen bonding, the RIC shows extremely high fracture toughness (16.43 kJ m^{-2}) and tear strength (9.63 kN m^{-1}), which can ensure coating integrity under various forms of stress, such as mechanical loading and harsh environments. As a result, RIC remains icephobic even after 35 icing/deicing cycles and 600 mechanical abrasions. The hydrogen bonding sites of RIC can also form hydrogen bonds with various substrates (Fig. 1), thus enhancing interfacial adhesion. Consequently, the chopped small piece of RIC keeps adhering to the substrate after ice adhesion testing. In addition, the reversible nature of the hydrogen bonding endows the RIC with self-healing properties, which helps to recover the coating from cuts and abrasions. RIC also demonstrates stability during saltwater immersion, and exposure to near-arctic weather (in Trondheim, Norway). This work introduces a toughening mechanism into soft icephobic coating and uses hydrogen bonding to enhance substrate adhesion of icephobic coating for the first time.

EXPERIMENTAL SECTION

Preparation

Synthesis of RIC solution

The synthesis route of RIC is shown in Fig. S1. Bis(3-aminopropyl)-terminated PDMS (NH_2-PDMS-NH_2, 25.000 g, 5 mmol, 100–120 cst, DMS-A21, Gelest) in tetrahydrofuran (THF, 50 mL, Sigma-Aldrich) was dropwise added into isophorone diisocyanate (IDI, 2.2228 g, 10 mmol, Sigma-Aldrich) in THF (15 mL) under vigorous stirring, and then stirred for 2 h. Afterward, 1,2-bis(2-aminoethoxy)ethane (0.741 g, 5 mmol, Sigma-Aldrich) in THF (10 mL) was added into the mixture under vigorous stirring and kept stirring at room temperature for two days before further preparation and testing.

Preparation of RIC

RICs with different thicknesses were prepared by solvent casting. The above solution or diluted solution (Table S1) was poured onto a glass surface, which was installed into a homemade mold [25], and then covered by Petri dishes and allowed to dry under ambient conditions for three days.

Preparation of spongy RIC (RIC-S)

RIC-S was prepared by using the template method [29]. Edible fine salt was kneaded by spraying water, cast in a cuboid mold to shape the salt template into a size of 6 cm × 6 cm × ~0.15 mm, and dried at 80°C for 6 h. Then 10 mL of the above RIC solution was diluted by 15 mL of THF. Afterward, 15 mL of the diluted

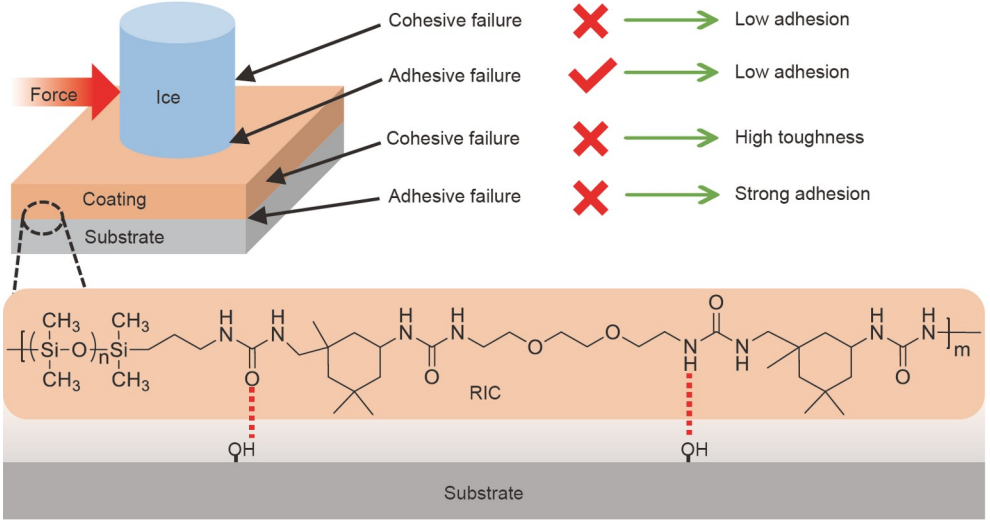

Figure 1 Design principle of an RIC. (i) Cohesive failure of ice, (ii) adhesive failure between ice and the coating, (iii) cohesive failure of the coating, or (iv) adhesive failure between the coating and substrate, may occur during ice removal. Supramolecular silicone, forming the basis of the RIC, contains hydrogen bonding sites leading to high toughness and the possible formation of hydrogen bonds with the substrate. This prevents the occurrence of cohesive failure in the coating, and adhesive failure at the coating-substrate interface.

solution was poured into the mold. After evaporation for three days, the salt-RIC mixture was demolded. To remove the salt, the salt-RIC mixture was then soaked in deionized water with ultrasonic treatment. The water was changed every day. After 3-day treatment, RIC-S was then dried at room temperature and adhered to the glass surface by using RIC solution. The as-prepared RIC showed a thickness of 1722 ± 30 μm.

Preparation of Sylgard 184 coating

Sylgard 184 coatings (base/curing agent: 10/1) with different thicknesses were prepared by drip coating or spin coating (Table S1). The coatings were cured at 65°C for 4 h.

Characterization

The molecular structure of RIC was confirmed by ^{1}H nuclear magnetic resonance (NMR, Bruker Avance III 400 MHz) and Fourier transform infrared (FT-IR, Thermo Nicolet Nexus FT-IR spectrometer). Water contact angles (WCAs) were measured on a drop shape analyzer (DSA100, KRÜSS). Deionized water (5 μL) was placed on the surface to obtain the static WCA. To measure the dynamic contact angles, 5 μL of deionized water was placed on the surface, followed by expanding and shrinking of deionized water at a rate of 0.1 mL min^{-1} *via* the needle of the syringe. Quasi-static nanoindentation measurement was conducted in TriboIndenter 950 (Hysitron, Inc.) by using a cono-spherical diamond indenter with a radius of 2.40 μm. The samples were loaded to the maximum load (75 μN) in 5 s, followed by holding for 2 s, and then unloading for another 5 s. Surface topography was recorded by atomic force microscopy (AFM, Bruker Dimension Icon) or there-dimensional (3D) optical profiler (Bruker). Optical microscopy images were recorded by a differential interference contrast (DIC) microscope (AxoScope A1, Carl Zeiss). Fracture toughness, tear strength, and shear strength of RIC to the different substrates were tested in an Instron mechanical testing system (model 5944). Fracture toughness was tested according to our previous report [33]. Tear strength was tested according to the standard ISO 34-1 by using a type of angle with a nick. For the shear strength of RIC to another different substrate, RIC solution was deposited onto a strip substrate (5 cm × 1 cm), followed by pressing another substrate above it with an overlapping area of (1 cm^2). After evaporation for two days, the specimen was subjected to a tensile test with a strain rate of 10 mm min^{-1}. The peak value was recorded and divided by the overlapping area to obtain the shear strength. Ice adhesion strength was tested by the vertical shear method at −10, −18, or −26°C with a velocity of 0.01 mm s^{-1} [25,28]. Deionized water (10 mL) was poured into a tube mold sealed on the coatings and kept at a specific temperature (−10, −18, or −26°C) for at least 4 h. Afterwards, the specimen was transferred into the testing chamber with a specific temperature (−10, −18 or −26°C) and stabilized for 15 min. During the test, the probe with a distance to the surface of ~1 mm propelled the ice cylinder at a velocity of 0.01 mm s^{-1}. The samples were abraded by a 400-grit sandpaper at a pressure of 1.5 kPa with a linear back-and-forth motion. The ice adhesion strength of the abraded sample was recorded every 200 cycles [35]. For the durability test, RIC samples were immersed in 1 mol L^{-1} saltwater as well as exposed to the outdoor environment in Trondheim, Norway from 15th Aug. 2020 to 15th Apr. 2021. Afterward, the samples were subjected to an ice adhesion test.

RESULTS AND DISCUSSION

The RIC polymer containing octuple hydrogen bonding was synthesized by a chain extension reaction according to our previous report (Fig. S1, preparation details are shown in Supplementary information (SI)) [33]. RIC and reference Sylgard 184 coatings with different thicknesses were prepared by solvent casting, drip coating, and spin coating (Table S1). The chemical structure of RIC was confirmed by ^{1}H NMR (Fig. S2) and FT-IR spectroscopy (Fig. S3). RIC shows high optical transmission (Fig. S4a), which makes it readily suitable for applications that require light transparency, such as windows, sensors, and solar panels.

It is known that surface wettability can affect the ice adhesion strength [36]. To study the wettability of different surfaces, we measured the static and dynamic WCAs of our RIC and commercial Sylgard 184 coatings (Fig. 2a and Fig. S5). As shown in Fig. 2, RIC shows a WCA of 112.1°, which is close to that of Sylgard 184 (115.1°), demonstrating the hydrophobicity and thus low surface energy of RIC. This is attributed to the identical backbone of RIC and Sylgard 184, which are mainly composed of PDMS. Their advancing contact angles (ACAs) also show similar values, while the receding contact angles (RCAs) exhibit a distinct difference. The RCA of RIC (48.1°) is ~38% lower than that of Sylgard 184 (77.2°), because of the presence of hydrophilic segments (ureido) in RIC. When the RIC is exposed to air, the PDMS parts tend to arrange themselves on the top of the surface to lower the surface energy. As the RIC contacts with water, the hydrophilic parts will rearrange to the water-coating interface, resulting in a lower RCA [37,38]. Nevertheless, at a lower temperature, the mobility of the molecular chain will be restricted, which will hinder the rearrangement of polymer chains. Hence, the lower receding WCA may not imply the higher work of adhesion at low temperatures.

To investigate the mechanical properties of the coatings, we used nanoindentation with a cono-spherical indenter (Fig. 2b and Table S2). The elastic moduli of the coatings can be obtained from the load-depth curves (Fig. 2b). The calculated values are 3.95 and 2.12 MPa for RIC and Sylgard 184, respectively. Values for the stiffness, reduced modulus, and hardness are also reported in Table S2. Although the elastic modulus of RIC is higher than that of Sylgard 184, it is still 2–3 orders of magnitude lower than that of ice [39]. Such a large mismatch in elastic modulus will result in deformation incompatibility at the interface during ice removal, which is in favor of the detachment of ice from the coating [24,29].

The influence of surface roughness on the ice adhesion strength is multifaceted [40]. The introduction of surface texture may increase the hydrophobicity of the surface; however, it may also lead to mechanical interlocking and increased ice adhesion strength [4]. The topography of RIC was obtained by AFM, as shown in Fig. 2c. Our RIC shows an ultra-smooth surface, with a root-mean-squared roughness of 0.567 nm (Table S2), effectively avoiding the mechanical interlocking between the formed ice and coating.

Toughness is the ability of a material to absorb energy up to the point of fracture. In this study, we used fracture toughness and tear strength to characterize the mechanical properties of RIC (Fig. 2d). For comparison, we also conducted the same tests for pure Sylgard 184. The fracture toughness was tested by the shear-test method, which has been widely used for soft materials [33]. As shown in Fig. 2d, the fracture toughness of RIC is

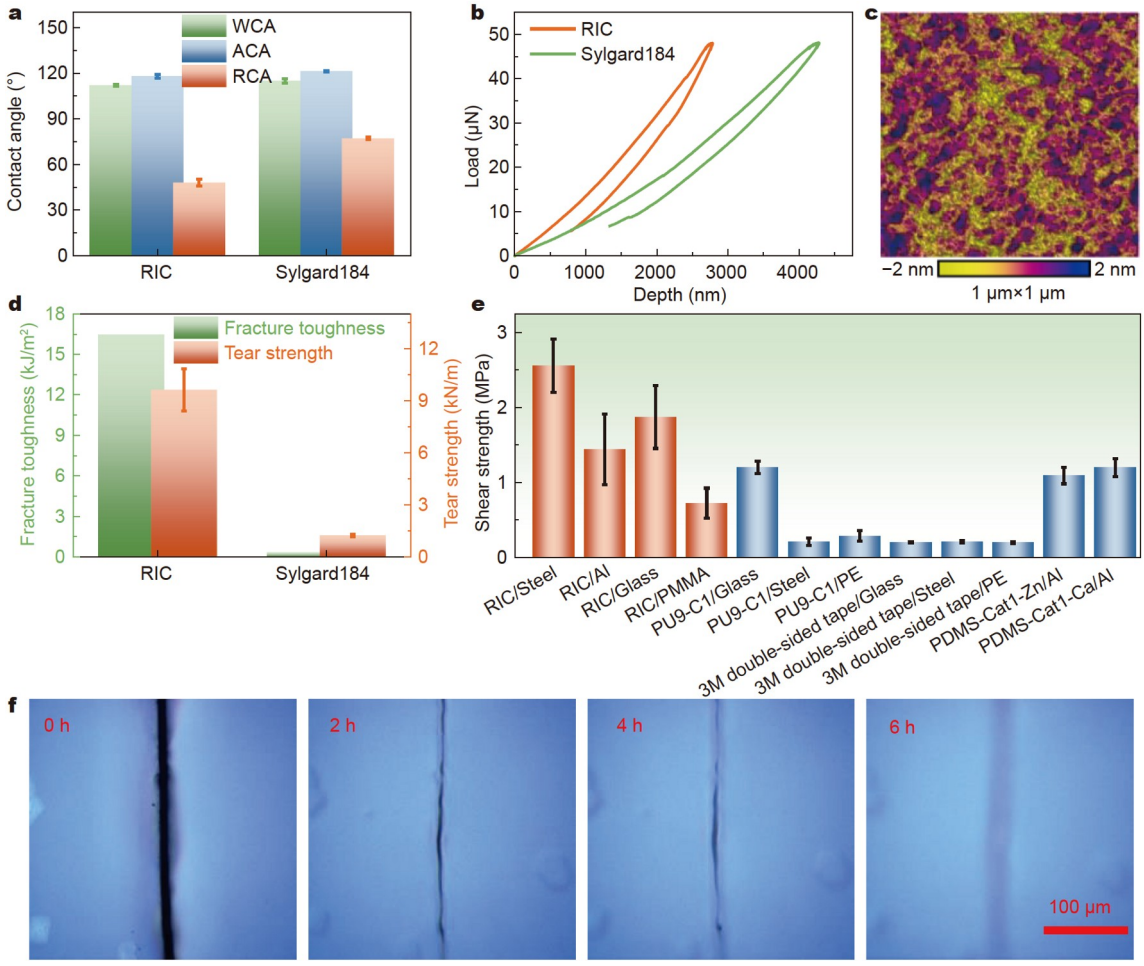

Figure 2 Characterizations of RIC and various reference materials. (a) Static WCAs, ACAs and RCAs of RIC and Sylgard 184. (b) Load-depth curves of RIC and Sylgard 184 obtained from nanoindentation. (c) AFM height image of RIC indicates an ultra-smooth surface. (d) Fracture toughnesses and tear strengths of RIC and Sylgard 184. (e) Shear strengths of RIC and reference materials on various substrates. Al: aluminium, PMMA: polymethyl methacrylate, PU9-C1: mucus-inspired supramolecular adhesives [32], PE: polyethylene, PDMS-Cat1-Zn: dual-cross-linked supramolecular polysiloxanes with zinc ion [41], PDMS-Cat1-Ca: dual-cross-linked supramolecular polysiloxanes with calcium ions [41]. (f) Self-healing process of RIC at 100°C.

16.43 kJ m^{-2}, ~46 times higher than that of Sylgard 184 (0.35 kJ m^{-2}). The tear strength was measured according to the testing standard ISO 34-1 by using an angle test piece with a nick. The tear strength of RIC is 9.63 kN m^{-1}, about 8 times higher than that of the commercial Sylgard 184 (1.24 kN m^{-1}). The high toughness of RIC is attributed to the octuple hydrogen bonding and the corresponding nanodomains, which can dissipate a large amount of energy under loading.

Supramolecular silicones have been demonstrated to strongly adhere to various substrates, which can avoid delamination in practical applications [30,31,41]. We evaluated the interfacial adhesion of our RIC to metal (steel and aluminum), inorganic non-metal (glass), and polymer (polymethyl methacrylate) surfaces by measuring the shear strength. As shown in Fig. 2e, the orange columns present the shear strength of RIC to the various surfaces. RIC exhibits significantly higher shear strength to these surfaces in comparison with the commercial 3M double-side tape and other reported supramolecular silicones [32,41]. Such a high adhesion strength is ascribed to the formation of hydrogen bonding between RIC and these surfaces.

Self-healing, one of the characteristics of many supramolecular polymers, has been introduced to enhance the mechanical durability of icephobic coatings [25,28]. Herein, we applied a cut in the RIC with a scalpel and let it heal at 100°C to study the healing process (Fig. 2f). The cut can be clearly observed by optical microscopy at the beginning of the healing process. As time elapses, the two edges of the coating move closer together. After 6 h, there is only a small visible indentation mark. The self-healing capability of RIC results from the flexibility of polymer chains and the reconfiguration of hydrogen bonds at the cut interface.

Ice adhesion strength has been widely used to evaluate icephobicity, which is defined as the ability of a surface to reach an ice adhesion strength below 100 kPa [42]. In this work, we characterized the ice adhesion strength of surfaces by the vertical shear test. As shown in Fig. 3a, the adhesion strength of ice to a bare glass surface is as high as 460.0 kPa. After being coated with RIC, the ice adhesion strength dramatically falls to 84.7 kPa, showing an 82% reduction. This value is slightly lower than the ice adhesion strength of commercial Sylgard 184 (103.5 kPa). The icephobicity of RIC results from the ultra-smoothness, low modulus, and low energy of the surface. During ice removal, the mismatch in elastic modulus between ice and RIC results in deformation incompatibility at the ice-RIC interface, conse-

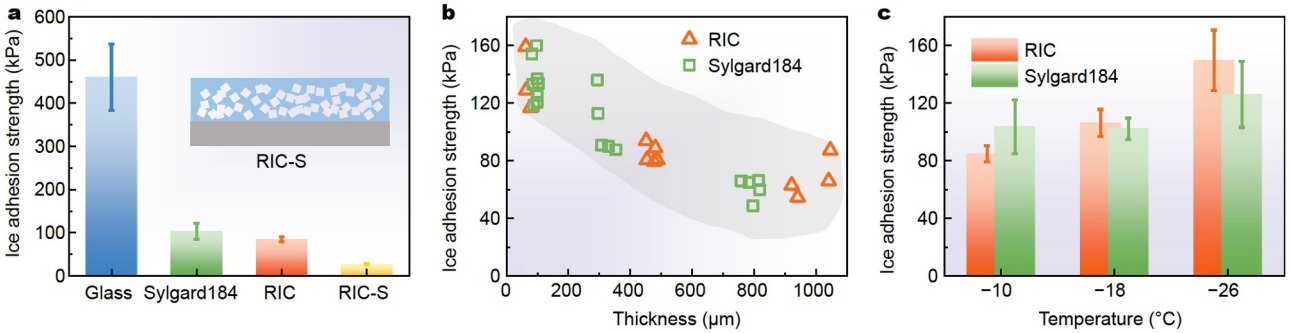

Figure 3 Ice adhesion strengths of RICs and reference surfaces. (a) Ice adhesion strengths of glass, Sylgard 184 (316 ± 22 μm), RIC (470 ± 15 μm), and RIC-S at −10°C. The inset illustrates the structure of RIC-S. (b) Ice adhesion strengths of RIC and Sylgard 184 coatings decrease with increasing coating thickness. All ice adhesion strengths were measured at −10°C. (c) Ice adhesion strengths of RIC (470 ± 15 μm) and Sylgard 184 (316 ± 22 μm) coatings increase with decreasing temperature.

quently inducing the interfacial voids. The formed voids can thus promote the adhesive failure of the ice-RIC interface [23]. In order to further reduce the ice adhesion strength, we prepared a coating with a spongy structure (RIC-S) as a representative demonstration by adopting a salt-based (NaCl) template, as shown in the inset of Fig. 3a. The spongy structure of RIC-S further decreases the elastic modulus of the coating, and in addition, such sub-structure promotes the deformation incompatibility, and thus the formation of cavities at the ice-coating interface, which will serve as macro crack initiators that further facilitate the detachment of ice [23,29]. As a result, the RIC-S presents a remarkable icephobicity, exhibiting a very low ice adhesion strength of 26.7 kPa.

To further investigate the influence of the coating thickness on the ice adhesion strength, we prepared RIC and Sylgard 184 coatings of different thicknesses (Table S1). As shown in Fig. 3b, the ice adhesion strengths of both RIC and Sylgard 184 show a reduction trend from ~160 to ~50 kPa with thickness increasing from ~80 to ~1000 μm. This trend coincides with the previous finding [43], i.e., increasing the soft coating thickness leads to a reduction in ice adhesion strength.

Since temperature is known to play an important role in the ice adhesion strength of coatings, the ice adhesion strengths of RIC and Sylgard 184 were measured at −10, −18, and −26°C [44]. As shown in Fig. 3c, Sylgard 184 shows an increase in ice adhesion strength from 103.5 to 126.1 kPa as the temperature drops from −10 to −26°C, while RIC exhibits an even more pronounced increase. This increase in ice adhesion strength is attributed to the increased number of hydrogen bonds at the interface, leading to a higher elastic modulus. Because of the presence of hydrogen bonding sites in RIC, the reduction of temperature will raise the number of hydrogen bonds between polymer chains, therefore inducing a more significant increase in modulus in comparison with Sylgard 184 [28]. Raising the temperature will increase the kinetic energy of molecules and thus lead to weakening hydrogen bonds. Hydrogen bonds are more stable and thus have a longer lifetime at low temperatures. For a certain period, the monitored number of hydrogen bonds should thus increase with decreasing temperature [45].

Besides the ice adhesion strength, durability is another key aspect in the field of icephobic materials [25]. As mentioned previously, one of the challenges in developing icephobic coatings is the combination of icephobicity and durability. Herein, the durability of RIC was investigated by monitoring the ice adhesion strength during icing/deicing cycles, cut/healing tests, abrasions, water immersion, saltwater immersion, and outdoor exposure. As shown in Fig. 4a, during 35 icing/deicing cycles, the ice adhesion strength stays below 80 kPa, because the high toughness helps to maintain coating integrity during ice removal.

Substrate adhesion is one of the critical parameters that can directly affect the coating's durability. To verify the strong adhesion of RIC to the substrate during deicing, we cut the coating into square pieces on the substrate (Fig. S4b) and then performed the ice adhesion test. During the test, the small square pieces under the ice will undergo the shear force. Without strong adhesion, delamination will occur instantaneously during deicing. The ice adhesion strength of the cut sample shows only a slight increase (Fig. 4b). Notably, the cut coating keeps adhering to the substrate after the ice adhesion test (Fig. 4c, upper photo), indicating excellent adhesion and the prevention of adhesive failure between the coating and substrate. Furthermore, thanks to the self-healing capability, the sample can fully self-repair the cut after four days of healing at 100°C (Fig. 4c, lower photo). Remarkably, the healed coating presents similar values of ice adhesion strength as the original coating.

To further study the mechanical durability of RIC, we measured the ice adhesion strength after mechanical abrasions [46]. The coating was subjected to linear back-and-forth motion of abrasion under the pressure of 1.5 kPa (Fig. S6), followed by the ice adhesion test every 200 abrasions. Notably, the ice adhesion strength of RIC keeps steady at around 80 kPa, even after 600 abrasions, because of the high toughness of the coating. After 800 abrasions, the ice adhesion strength of RIC increases to above 100 kPa. This loss of icephobicity is ascribed to the increased roughness and abrasion-induced ice interlocking. The RIC is rendered translucent after 1000 abrasions, because of the rough surface which scatters light to a greater extent, as shown in Fig. S4c. The roughnesses of the coating before and after 1000 abrasions were further characterized by 3D optical profilometry, as shown in Fig. 4e (left panel and middle panel). The surface becomes uneven after 1000 abrasions (Fig. 4e) with the root-mean-squared roughness increased from 7.9 to 1127 nm (Table S3). Unavoidably, such high roughness leads to mechanical interlocking during ice removal which increases the ice adhesion strength. Nevertheless, the abrased coating is capable of self-healing the damage induced by mechanical wear, as shown in Fig. S4d. The hazy abrasive RIC turns clearly trans-

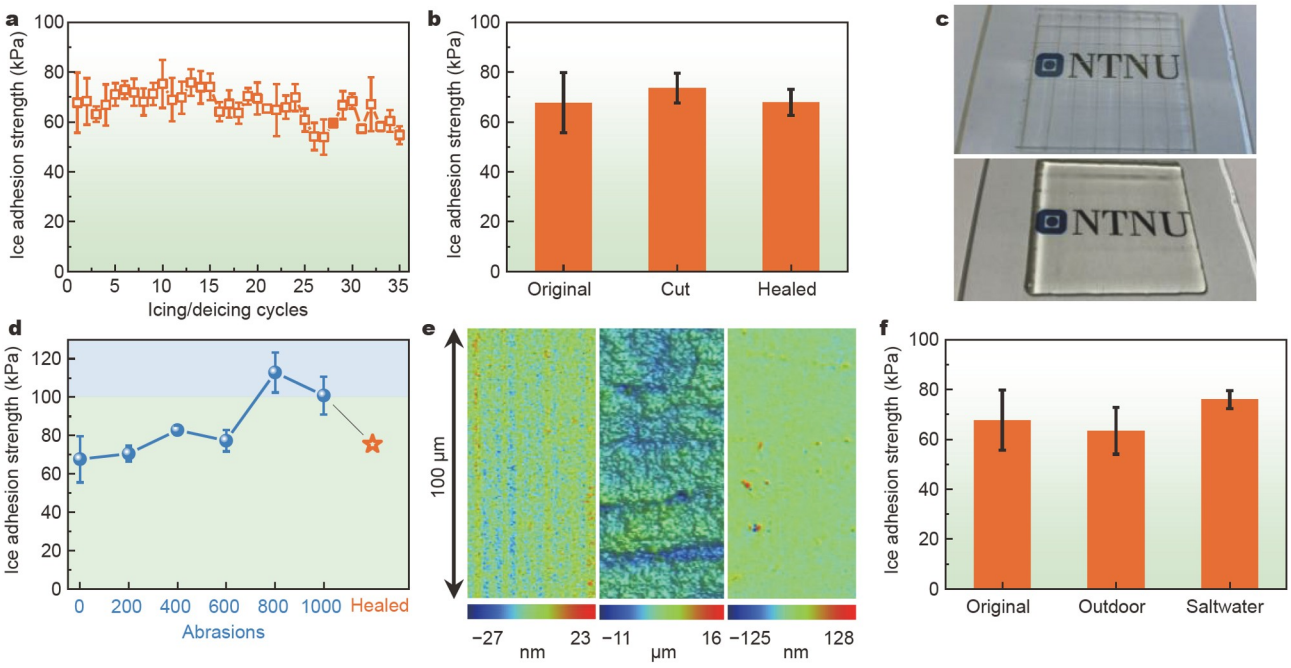

Figure 4 Durability tests of RIC. (a) Ice adhesion strengths of RIC during icing/deicing tests. RIC presents a stable ice adhesion of ~65 kPa during 35 icing/deicing cycles. (b) Ice adhesion strengths of RIC before cut, after the cut, and after self-healing. (c) RIC self-heals the cuts at 100°C for four days. The upper photo shows the cut sample after ice adhesion testing, while the lower photo shows the sample after self-healing. The coating was applied onto a 6 cm × 6 cm glass substrate. (d) Ice adhesion strengths of RIC during abrasion tests and after self-healing from abrasion (denoted by a red star). (e) Morphologies of RIC before abrasion (left), after 1000 abrasions (middle), and healed from abrasions (right), as characterized by the 3D optical profiler. (f) Ice adhesion strength of RIC keeps stable after outdoor exposure and saltwater immersion (Trondheim, Norway; from 15th Aug. 2020 to 15th Apr. 2021) for eight months.

parent after the healing process at 100°C for one day, due to the recovery of the surface smoothness (Fig. 4e, right panel). The root-mean-squared roughness decreases to nanoscale (19.4 nm). Such a smooth surface prevents mechanical interlocking, and hence the ice adhesion strength of repaired RIC returns to 75.5 kPa.

To verify the durability in a real environment, we conducted outdoor exposure of the RIC in Trondheim, Norway from 15th Aug. 2020 to 15th Apr. 2021 (i.e., through the summer, autumn, and winter periods). During the testing, the temperature and humidity changed, and factors such as solar radiation, dust contamination, and icing/deicing, are potential promoters for delamination, mechanical breakage, oxidation, and degradation of the coatings. Although undergoing such complex challenges, the RIC retains its icephobicity by presenting a low ice adhesion strength of 63.5 kPa (Fig. 4f). Furthermore, in the application for ship hull and marine infrastructure, the resistance of the coating to saltwater is also important. The ice adhesion strength of RIC after eight months of saltwater immersion stays at around 76.0 kPa, demonstrating remarkable stability in saltwater. The stability of the coating in a complex environment is attributed to the hydrophobicity, chemical inertness, toughness, as well as strong adhesion to the substrate. The hydrophobicity, resulting from the PDMS segments, diminishes the swelling of the coating under saltwater. The chemical inertness of the RIC inhibits chemical reactions during liquid immersion and weather exposure. At the same time, the mechanical toughness and strong adhesion prevent the breakage and delamination of the coating during liquid immersion and outdoor exposure. Hence, RIC can sustain severe mechanical loading and harsh environments.

CONCLUSIONS

In summary, we designed and fabricated an RIC possessing high toughness, strong adhesion to the substrate, and self-healing function. For the first time, we introduced the toughening mechanism to enhance the mechanical durability of soft icephobic coatings. RIC demonstrated high fracture toughness (16.43 kJ m^{-2}) and tear strength (9.63 kN m^{-1}), due to the incorporated octuple hydrogen bonding, which also gives a strong interaction with the substrate. The prominent toughness and strong adhesion to various substrates endow the coating with the capability to withstand multiple icing/deicing cycles, mitigate the effect of mechanical abrasions, and avoid coating delamination. Consequently, RIC maintains its icephobicity after 35 icing/deicing cycles and 600 sandpaper abrasions, while maintaining its excellent optical transparency. In addition, the RIC presents a self-healing capacity owing to the dynamic hydrogen bonds, and can thus self-repair mechanical damage such as cuts and abrasions to recover its icephobicity. Furthermore, the RIC also displays remarkable stability in the complex harsh environment, such as weather exposure and saltwater immersion. This work can not only guide the development of durable icephobic coatings but also inspire the design of other protective coatings (anti-fouling, anti-corrosion, etc.) towards high durability in complex harsh environments.

Received 1 September 2022; accepted 25 November 2022; published online 14 February 2023

1 Zhuo Y, Xiao S, Amirfazli A, *et al.* Polysiloxane as icephobic materials—The past, present and the future. Chem Eng J, 2021, 405: 127088

2 Golovin K, Dhyani A, Thouless MD, *et al.* Low-interfacial toughness materials for effective large-scale deicing. Science, 2019, 364: 371–375
3 Azimi Dijvejin Z, Jain MC, Kozak R, *et al.* Smart low interfacial toughness coatings for on-demand de-icing without melting. Nat Commun, 2022, 13: 5119
4 Shen Y, Wu X, Tao J, *et al.* Icephobic materials: Fundamentals, performance evaluation, and applications. Prog Mater Sci, 2019, 103: 509–557
5 Kreder MJ, Alvarenga J, Kim P, *et al.* Design of anti-icing surfaces: Smooth, textured or slippery? Nat Rev Mater, 2016, 1: 15003
6 Sojoudi H, Wang M, Boscher ND, *et al.* Durable and scalable icephobic surfaces: Similarities and distinctions from superhydrophobic surfaces. Soft Matter, 2016, 12: 1938–1963
7 Jamil MI, Ali A, Haq F, *et al.* Icephobic strategies and materials with superwettability: Design principles and mechanism. Langmuir, 2018, 34: 15425–15444
8 Liu J, Zhu C, Liu K, *et al.* Distinct ice patterns on solid surfaces with various wettabilities. Proc Natl Acad Sci USA, 2017, 114: 11285–11290
9 Wang Y, Yao X, Chen J, *et al.* Organogel as durable anti-icing coatings. Sci China Mater, 2015, 58: 559–565
10 Alasvand Zarasvand K, Orchard D, Clark C, *et al.* Effect of curvature on durable ice-phobic surfaces based on buckling metallic plates. Mater Des, 2022, 220: 110884
11 Wang L, Gong Q, Zhan S, *et al.* Robust anti-icing performance of a flexible superhydrophobic surface. Adv Mater, 2016, 28: 7729–7735
12 Hejazi V, Sobolev K, Nosonovsky M. From superhydrophobicity to icephobicity: Forces and interaction analysis. Sci Rep, 2013, 3: 2194
13 Subramanyam SB, Kondrashov V, Rühe J, *et al.* Low ice adhesion on nano-textured superhydrophobic surfaces under supersaturated conditions. ACS Appl Mater Interfaces, 2016, 8: 12583–12587
14 Liu B, Zhang K, Tao C, *et al.* Strategies for anti-icing: Low surface energy or liquid-infused? RSC Adv, 2016, 6: 70251–70260
15 Farhadi S, Farzaneh M, Kulinich SA. Anti-icing performance of superhydrophobic surfaces. Appl Surf Sci, 2011, 257: 6264–6269
16 Kulinich SA, Farhadi S, Nose K, *et al.* Superhydrophobic surfaces: Are they really ice-repellent? Langmuir, 2011, 27: 25–29
17 Subramanyam SB, Rykaczewski K, Varanasi KK. Ice adhesion on lubricant-impregnated textured surfaces. Langmuir, 2013, 29: 13414–13418
18 He Z, Xie WJ, Liu Z, *et al.* Tuning ice nucleation with counterions on polyelectrolyte brush surfaces. Sci Adv, 2016, 2: e1600345
19 Zhu T, Cheng Y, Huang J, *et al.* A transparent superhydrophobic coating with mechanochemical robustness for anti-icing, photocatalysis and self-cleaning. Chem Eng J, 2020, 399: 125746
20 He Z, Wu C, Hua M, *et al.* Bioinspired multifunctional anti-icing hydrogel. Matter, 2020, 2: 723–734
21 Zhuo Y, Xiao S, Håkonsen V, *et al.* Anti-icing ionogel surfaces: Inhibiting ice nucleation, growth, and adhesion. ACS Mater Lett, 2020, 2: 616–623
22 Bai G, Gao D, Liu Z, *et al.* Probing the critical nucleus size for ice formation with graphene oxide nanosheets. Nature, 2019, 576: 437–441
23 He Z, Xiao S, Gao H, *et al.* Multiscale crack initiator promoted superlow ice adhesion surfaces. Soft Matter, 2017, 13: 6562–6568
24 Beemer DL, Wang W, Kota AK. Durable gels with ultra-low adhesion to ice. J Mater Chem A, 2016, 4: 18253–18258
25 Zhuo Y, Håkonsen V, He Z, *et al.* Enhancing the mechanical durability of icephobic surfaces by introducing autonomous self-healing function. ACS Appl Mater Interfaces, 2018, 10: 11972–11978
26 Golovin K, Tuteja A. A predictive framework for the design and fabrication of icephobic polymers. Sci Adv, 2017, 3: e1701617
27 Rønneberg S, He J, Zhang Z. The need for standards in low ice adhesion surface research: A critical review. J Adhes Sci Tech, 2019, 34: 319–347
28 Zhuo Y, Xiao S, Håkonsen V, *et al.* Ultrafast self-healing and highly transparent coating with mechanically durable icephobicity. Appl Mater Today, 2020, 19: 100542
29 He Z, Zhuo Y, He J, *et al.* Design and preparation of sandwich-like polydimethylsiloxane (PDMS) sponges with super-low ice adhesion. Soft Matter, 2018, 14: 4846–4851
30 Liu M, Wang Z, Liu P, *et al.* Supramolecular silicone coating capable of strong substrate bonding, readily damage healing, and easy oil sliding. Sci Adv, 2019, 5: eaaw5643
31 Cao C, Yi B, Zhang J, *et al.* Sprayable superhydrophobic coating with high processibility and rapid damage-healing nature. Chem Eng J, 2020, 392: 124834
32 He W, Wang Z, Hou C, *et al.* Mucus-inspired supramolecular adhesives with oil-regulated molecular configurations and long-lasting antibacterial properties. ACS Appl Mater Interfaces, 2020, 12: 16877–16886
33 Zhuo Y, Xia Z, Qi Y, *et al.* Simultaneously toughening and stiffening elastomers with octuple hydrogen bonding. Adv Mater, 2021, 33: 2008523
34 Song P, Wang H. High-performance polymeric materials through hydrogen-bond cross-linking. Adv Mater, 2020, 32: 1901244
35 Zhuo Y, Li T, Wang F, *et al.* An ultra-durable icephobic coating by a molecular pulley. Soft Matter, 2019, 15: 3607–3611
36 Meuler AJ, Smith JD, Varanasi KK, *et al.* Relationships between water wettability and ice adhesion. ACS Appl Mater Interfaces, 2010, 2: 3100–3110
37 Inutsuka M, Yamada NL, Ito K, *et al.* High density polymer brush spontaneously formed by the segregation of amphiphilic diblock copolymers to the polymer/water interface. ACS Macro Lett, 2013, 2: 265–268
38 Yanagi K, Yamada NL, Kato K, *et al.* Polyrotaxane brushes dynamically formed at a water/elastomer interface. Langmuir, 2018, 34: 5297–5302
39 Langleben MP. Young's modulus for sea ice. Can J Phys, 1962, 40: 1–8
40 Nosonovsky M, Hejazi V. Why superhydrophobic surfaces are not always icephobic. ACS Nano, 2012, 6: 8488–8491
41 Yi B, Liu P, Hou C, *et al.* Dual-cross-linked supramolecular polysiloxanes for mechanically tunable, damage-healable and oil-repellent polymeric coatings. ACS Appl Mater Interfaces, 2019, 11: 47382–47389
42 Golovin K, Kobaku SPR, Lee DH, *et al.* Designing durable icephobic surfaces. Sci Adv, 2016, 2: e1501496
43 Wang C, Fuller T, Zhang W, *et al.* Thickness dependence of ice removal stress for a polydimethylsiloxane nanocomposite: Sylgard 184. Langmuir, 2014, 30: 12819–12826
44 Boinovich LB, Emelyanenko KA, Emelyanenko AM. Superhydrophobic *versus* slips: Temperature dependence and the stability of ice adhesion strength. J Colloid Interface Sci, 2022, 606: 556–566
45 Skrovanek DJ, Howe SE, Painter PC, *et al.* Hydrogen bonding in polymers: Infrared temperature studies of an amorphous polyamide. Macromolecules, 1985, 18: 1676–1683
46 Jia C, Chen C, Mi R, *et al.* Clear wood toward high-performance building materials. ACS Nano, 2019, 13: 9993–10001

Acknowledgements This work was financially supported by the Research Council of Norway *via* the PETROMAKS2 Project Durable Arctic Icephobic Materials (255507), the NANO2021 Project Dual-Functional Anti-Gas Hydrate Surfaces (302348) and the Norwegian Micro- and Nano-Fabrication Facility, NorFab (245963). Li T thanks the support of the National Natural Science Foundation of China (12002350).

Funding note Open Access funding provided by NTNU Norwegian University of Science and Technology (incl St. Olavs Hospital-Trondheim University Hospital).

Author contributions Zhuo Y designed the experiments and wrote the paper; Zhuo Y, Liu S, Wang F, and Luo S conducted the experiments and characterizations. Håkonsen V, Li T, and Xiao S analyzed the data and reviewed the paper. He J and Zhang Z analyzed the data and wrote the paper. All authors contributed to the general discussion.

Conflict of interest The authors declare that they have no conflict of interest.

Supplementary information Supporting data are available in the online version of the paper.

Yizhi Zhuo completed his Bachelor's degree in applied chemistry at the South China University of Technology in 2013, and then his Master's degree in chemical engineering at Xiamen University in 2016. In 2019, he received his PhD degree from the Norwegian University of Science and Technology (NTNU), where he worked on designing durable icephobic materials. His research focuses on designing and synthesizing soft materials for anti-icing and exploring the underlying mechanisms.

Jianying He received her PhD degree in structural engineering from the NTNU in 2009. She was an assistant professor at the University of Science and Technology Beijing (2003–2006), a postdoctoral fellow at NTNU (2009–2011), and an associate professor at NTNU (2011–2017), and became a professor in nanomechanics at NTNU in 2017. Her current research area includes nanostructured materials, nanotechnology for petroleum engineering, and nano-enabled icephobicity.

Zhiliang Zhang received his PhD degree from the Lappeenranta University of Technology in 1994. He then worked at SINTEF Materials and Chemistry, Trondheim, before he was appointed as a full professor at the NTNU in 2003. He is an elected member of the Norwegian Academy of Technological Sciences and an editor-in-chief for *Engineering Fracture Mechanics*. He currently focuses on anti-adhesive materials, nano-structured functional materials for energy applications, and fracture mechanics.

超耐用疏冰涂层的制备及性能研究

卓毅智[1,5*], Verner Håkonsen[2], 刘思琪[1], 李彤[3], 王锋[1], 罗四海[4], 肖森波[1], 何健英[1*], 张志良[1*]

摘要 被动疏冰涂层作为一种新形防除冰方法，拥有环境友好、耗能低、经济等优势，因此在过去十几年来被广泛研究. 但是，目前的主动疏冰涂层仍存在疏冰性与耐久性难以兼容的问题. 本文设计了一种兼具高韧性、强基底粘附力和自愈合能力的透明疏冰涂层. 涂层具有疏水性、光滑表面及低模量，保障了涂层的低冰粘附强度. 通过引入类海绵结构，冰粘附强度可降低至26.7 ± 1.1 kPa. 涂层高分子网络的多重氢键赋予其高韧性、强基底粘附力和自愈合能力. 因此，涂层在35次结冰/除冰循环和600次机械磨损之后能避免涂层剥离并保持疏冰性，且能愈合机械磨损恢复其疏冰性. 另外，涂层在海水及近北极气候暴露8个月后仍能保持良好的疏冰性. 该工作为耐久性疏冰涂层的设计提供了一种新思路.

